

Binding Studies of Isoxsuprine Hydrochloride to Calf Thymus DNA Using Multispectroscopic and Molecular Docking Techniques

Sadegh Salehzadeh¹ · Farshid Hajibabaei² · Neda Hosseinpour Moghadam¹ · Samira Sharifinia¹ · Sadegh Khazalpour¹ · Reza Golbedaghi²

Received: 5 June 2017 / Accepted: 2 October 2017 / Published online: 6 October 2017
© Springer Science+Business Media, LLC 2017

Abstract In the present work, the interaction of Isoxsuprine (ISX) with Calf thymus DNA (ct-DNA) under physiological conditions (Tris–HCl buffer of pH 7.4) was investigated by using electronic absorption, circular dichroism, viscosity, electrochemical studies, fluorescence techniques, salt effect studies and computational studies. Competitive fluorimetric studies with Hoechst 33258 have shown that ISX exhibit the ability to displace the DNA-bound Hoechst 33258, indicating that it binds to ct-DNA in strong competition with Hoechst 33258 for the minor groove binding. Furthermore, the resulting data showed that ISX cannot displace methylene blue or acridine orange, which are the common intercalator molecules. The viscosity of ct-DNA solution was almost unchanged on addition of ISX and circular dichroism (CD) spectra of ct-DNA showed small changes in the presence of ISX which is in agreement with groove binding mode of interaction. Thus all above studies showed that the ISX drug binds to ct-DNA in a groove binding mode. The salt-effect studies showed the non-electrostatic nature of binding of ISX to ct-DNA. Moreover, molecular docking results support the above experimental data and suggest that ISX prefers to bind on the minor groove of ct-DNA.

Keywords Isoxsuprine · DNA interaction · Molecular docking · DFT · Groove binding

Introduction

Recent years have seen a rejuvenation of interest in studies on the interaction mechanism of deoxyribonucleic acid (DNA) with small molecules, especially in interaction with drugs [1–5], chemical composition of plant extracts [6] and coordination compounds [7]. The dominant binding class of small molecules with DNA can be classified as (i) covalent binding and (ii) non-covalent binding (electrostatic binding, groove binding or intercalation). Study on binding modes and binding properties of drugs to DNA can help us to rationally design new drugs [8–10].

Isoxsuprine (ISX), 4-hydroxy- α -[1-[(1-methyl-2-phenoxyethyl) amino] ethyl] benzenemethanol (Fig. 1), has been used in the cure of cerebral and peripheral vascular disease, and arresting the premature labor [11].

Herein, we want to study the mode of the interaction between ISX and DNA. Obviously, such studies will help us to know more about the mechanism of damaging DNA in the presence of latter drug. In order to investigate the binding properties of ISX with ct-DNA we used multiple spectroscopic techniques such as electronic absorption spectroscopy, fluorescence techniques and circular dichroism spectroscopy. Salt effect studies, electrochemical studies, and dynamic viscosity measurements were also used. In addition, molecular docking simulations were performed.

Experimental Details

Materials and Methods

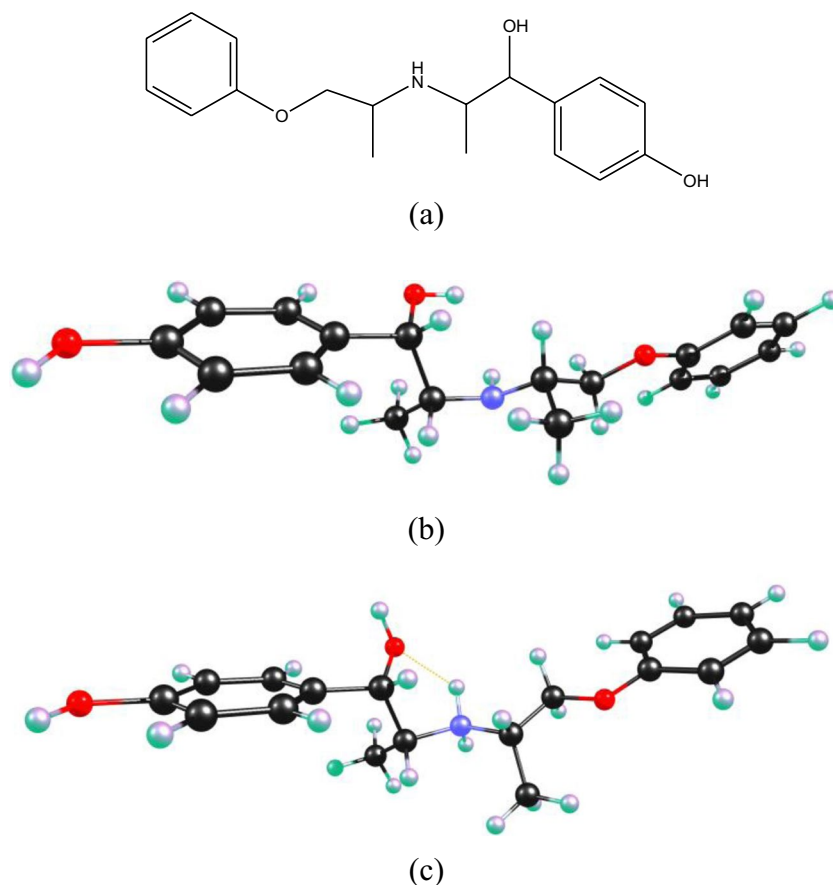
The highly polymerized ct-DNA, ISX, Methylene blue (MB), Acridine orange (AO), Hoechst 33258, and Tris–HCl were purchased from Sigma company. Tris–HCl

✉ Sadegh Salehzadeh
ssalehzadeh@gmail.com

¹ Faculty of Chemistry, Bu-Ali Sina University, Hamedan, Iran

² Chemistry Department, Payame Noor University, 19395-4697 Tehran, Iran

Fig. 1 The chemical structure of ISX (a) and optimized structures of ISX (b) and its protonated form (c) at BP86/def2-tzvp level of theory



buffer solution having a pH of 7.4 was prepared from Tris-(hydroxymethyl)-amino-methane-hydrogen chloride. Stock solution of ct-DNA was prepared by dissolving about 1–2 mg of ct-DNA fibers in Tris-HCl buffer (2 ml, 10 mM) and stored for 24 h at 4 °C. The concentration of ct-DNA in stock solution (1×10^{-3} M) was expressed in monomer units, as determined by UV absorption at 260 nm using a molar absorption coefficient (ϵ_p) of $6600 \text{ M}^{-1} \text{ cm}^{-1}$. ct-DNA solutions were used after no more than 4 days. For Tris-buffer solution of ct-DNA the ratio of UV absorbance at 260 and 280 nm was about 1.8, indicating that the ct-DNA is adequately free from protein contamination. ISX stock solution (1×10^{-3} M) was prepared by dissolving a required amount of Isoxsuprine hydrochloride (ISX-HCl) in Tris-HCl buffer.

Instrumentation

Absorbance spectra were recorded on an Analytik Jena Specord 210 spectrophotometer using a quartz cell with 1.0 cm path length. The absorbance measurements were performed by keeping the concentration of ISX constant (5×10^{-5} M) while varying that of ct-DNA from 0 to 6.5×10^{-5} M. Absorbance of DNA blank used as control for all of measurements. The samples were incubated for 30 min, and the spectra were recorded in the range of

200–320 nm. CD measurements were recorded on a JASCO (J-810) spectropolarimeter, using a quartz cell with 1.0 cm path length and by keeping the concentration of ct-DNA constant (8×10^{-5} M) while varying the ISX concentration ($0.0\text{--}1.5 \times 10^{-4}$ M). Viscosity measurements were made with a SCHOT AVS 450 viscosimeter maintained at $25 \text{ }^\circ\text{C} \pm 0.5 \text{ }^\circ\text{C}$. The ct-DNA concentration was fixed at 5×10^{-5} M, the flow time was measured with a digital stopwatch and the viscosity η of the samples was evaluated from the mean value of three measurements. The values of relative specific viscosity $(\eta/\eta_0)^{1/3}$, where η_0 and η are the specific viscosity contributions of ct-DNA in the absence and in the presence of the ISX, respectively, were plotted against $1/R$ ($R = [\text{ISX}] / [\text{DNA}] = 0.0$ to 2.9).

Fluorescence measurements were carried out by using a JASCO FP 6200 spectrofluorometer. Binding location of ISX in DNA was studied in the presence of three probes (Hoechst 33258, MB and AO) using the fluorescence titration method. The concentration of probe and DNA were fixed, and ISX-HCl was gradually added to the mixtures ($[\text{ISX}] = 0.0\text{--}17.7 \times 10^{-5}$ M). The fluorescence spectra of different mixtures were recorded over a wavelength range of 370–515 nm ($\lambda_{\text{ex}} = 340$ nm), 640–750 nm ($\lambda_{\text{ex}} = 620$ nm) and 470–650 nm ($\lambda_{\text{ex}} = 464$ nm) in the cases of Hoechst 33258, MB and AO, respectively.

The cyclic voltammetric measurements were performed using an Autolab model PGSTAT 302n potentiostat/galvanostat. The working electrode used in above measurements was a glassy carbon disk (1.8 mm² area) where a platinum wire was used as a counter electrode. The working electrode potentials were measured versus Ag/AgCl electrode (from AZAR electrode and Metrohm) as reference electrode and a Pt wire as counter electrode. Electrochemical experiments were performed in a 25-mL voltammetric cell at room temperature. All potentials are referred to the Ag/AgCl reference. The surfaces of all working electrodes were freshly polished with 0.05 mm alumina prior to each experiment and were rinsed between each polishing step. The supporting electrolyte was 0.01 M of Tris–HCl buffer solution (pH 7.4). The current–potential curves and experimental data were recorded on software GPES.

Computational Details

The structure of ISX and its protonated form were optimized using the BP86 functional [12, 13]. The def2-TZVP [14] basis set was employed for all atoms and structures were optimized without symmetry restrictions. All calculations were performed using the Gaussian 03 set of programs [15].

The optimized structure of ISX and its protonated form were used for the molecular docking calculations Fig. 1. The crystal structures of 1BNA used in molecular docking were extracted from Protein Data Bank (<http://www.rcsb.org/pdb/home/home.do>).

The binding interactions of ISX and its protonated form with 1BNA were simulated by molecular docking method using AutoDock 4.0 program [16]. The polar hydrogen atoms were added to 1BNA and the rotatable bonds of ISX and its protonated form were set to using Autodock Tools

[17, 18]. The grid maps of dimensions 60×60×60 Å with a grid-point spacing of 0.375 Å were created for 1BNA to ensure that there is an appropriate space for ISX and its protonated form. Other miscellaneous parameters were assigned the default values given by the Autodock program. The dominating configuration of the binding complexes of ISX and its protonated form with NDA having the minimum binding free energy (ΔG) were finally obtained.

Results and Discussion

Electronic Absorption Spectroscopy

Electronic absorption spectroscopy is an effective technique to study the interaction between drug molecules and ct-DNA by monitoring possible changes in absorption intensity and position of the bands. The absorption spectra were recorded with the fixed-concentration of ISX (5×10^{-5} M) and different concentrations of ct-DNA (0 – 3.0×10^{-5} M) and resulting spectra are displayed in Fig. 2. The absorption intensity of ISX decreased slightly with consecutive additions of ct-DNA solution, indicating that there is an attractive interaction between ISX and ct-DNA which is not consistent with the intercalation binding mode. From the absorption intensity data, the intrinsic binding constant K_b was calculated using the Eq. (1) [19].

$$\frac{[DNA]}{(\epsilon_a - \epsilon_f)} = \frac{[DNA]}{(\epsilon_b - \epsilon_f)} + \frac{1}{K_b(\epsilon_b - \epsilon_f)} \quad (1)$$

Where, [DNA] is the concentration of ct-DNA and ϵ_a , ϵ_f and ϵ_b correspond to the apparent molar absorption coefficient, the molar absorption coefficient for the free drug and its entirely ct-DNA-bound combination, respectively. The binding

Fig. 2 Absorption spectra of ISX in the presence of ct-DNA at different concentrations. Conditions: $c(\text{ISX}) = 5 \times 10^{-5}$ mol L⁻¹. $c(\text{DNA})(\times 10^{-5}$ mol L⁻¹): 0.0, 0.5, 1.0, 1.5, 2.0, 2.5, 3.0 and pH=7.4

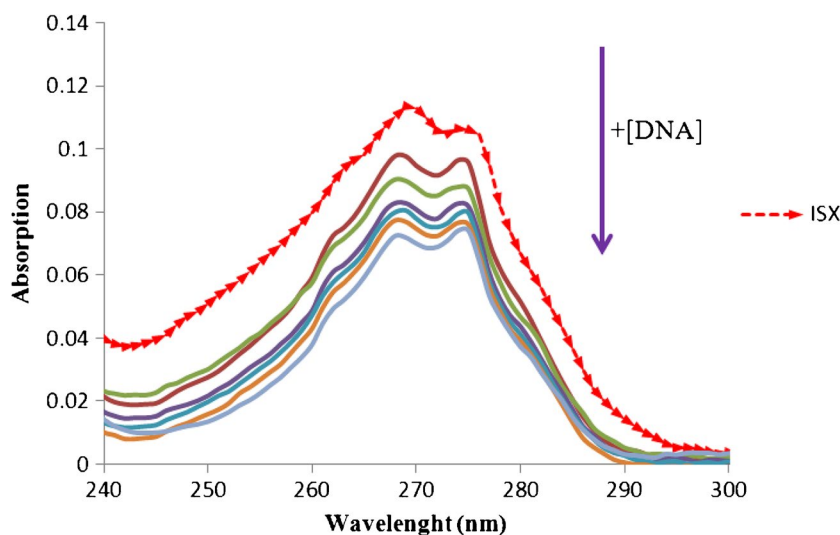


Fig. 3 Plots of $[DNA]/\epsilon_a - \epsilon_f$ vs. $[DNA]$ for the binding of ISX and ct-DNA

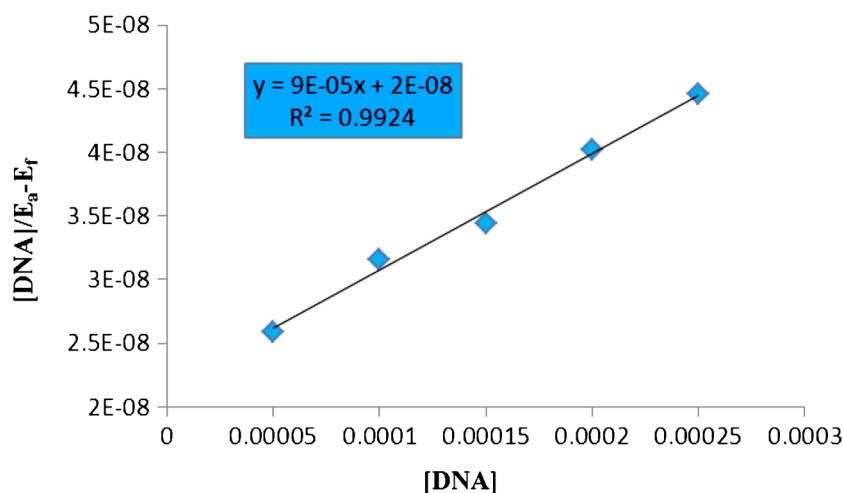
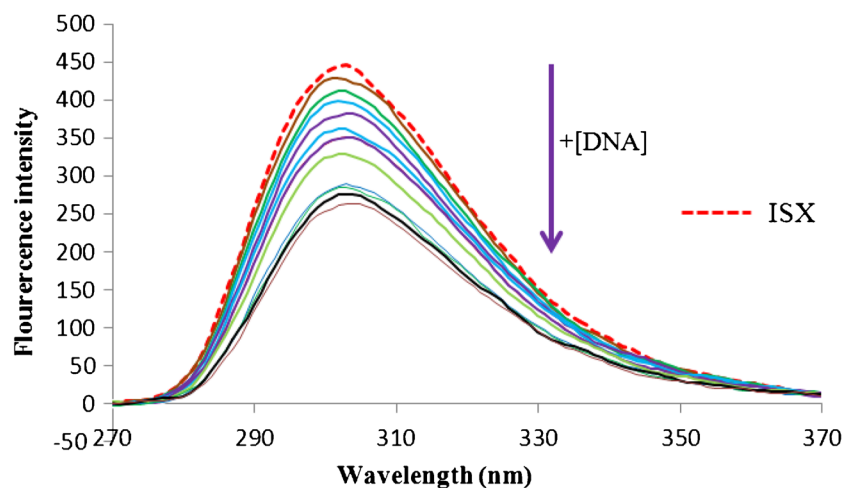


Fig. 4 Fluorescence spectra of ISX in the presence of ct-DNA at different concentrations (pH = 7.4, T = 298 K, $\lambda_{ex} = 242$ nm, $c(\text{ISX}) = 5 \times 10^{-5}$ mol L⁻¹, $c(\text{ct-DNA}) = 0.0, 1.9, 3.9, 5.9, 7.8, 9.8, 11.8, 13.7, 15.7, 17.7, 19.7, 21.6$ and 23.6×10^{-5} mol L⁻¹ for curves 1e12, respectively)



constant (K_b) was obtained by the ratio of the slope to intercept in the plots of $[DNA] / (\epsilon_a - \epsilon_f)$ versus $[DNA]$ (Fig. 3), which was estimated to be 4.5×10^3 M⁻¹ for ISX.

Fluorescence Quenching Studies

ISX demonstrated a strong fluorescence emission band centered at 301 nm when excited at 242 nm. The fluorescence emission spectra of ISX in the absence and presence of different concentrations of ct-DNA are shown in Fig. 4. As can be seen, a regular decrease in fluorescence intensity of ISX is observed with addition of different concentrations of ct-DNA, indicating that ct-DNA quenches the intrinsic fluorescence of ISX.

The quenching rate constant (k_q) for the excited states of ISX was determined according to Stern–Volmer equation:

$$\frac{F_0}{F} = 1 + K_q \tau_0 [Q] = 1 + K_{SV} [Q] \quad (2)$$

Table 1 The quenching constants of ISX by ct-DNA at different temperatures

T (K)	R ²	K_{SV} (L mol ⁻¹) $\times 10^3$	K_q (L mol ⁻¹) $\times 10^{11}$
283	0.99	2.18	2.18
288	0.97	1.96	1.96
298	0.98	1.79	1.79
310	0.98	1.51	1.51

In Eq. (2) F_0 and F are the fluorescence intensities in the absence and presence of different concentrations of ct-DNA. K_{SV} is the Stern–Volmer quenching constant, $[Q]$ is the concentration of ct-DNA and τ_0 is the average fluorescence lifetime ($\sim 10^{-8}$ s) [20]. Generally, quenching data are usually presented as plots of F_0/F versus $[Q]$ and the values of K_{SV} and K_q at different temperatures are given in Table 1. The values of K_q were significantly higher than that of the maximum scattering collision quenching constant (2.0×10^{10}

Fig. 5 The Plots of $\log(F_0 - F)/F$ versus $\log[Q]$ for the binding of ISX with ct-DNA at different temperatures

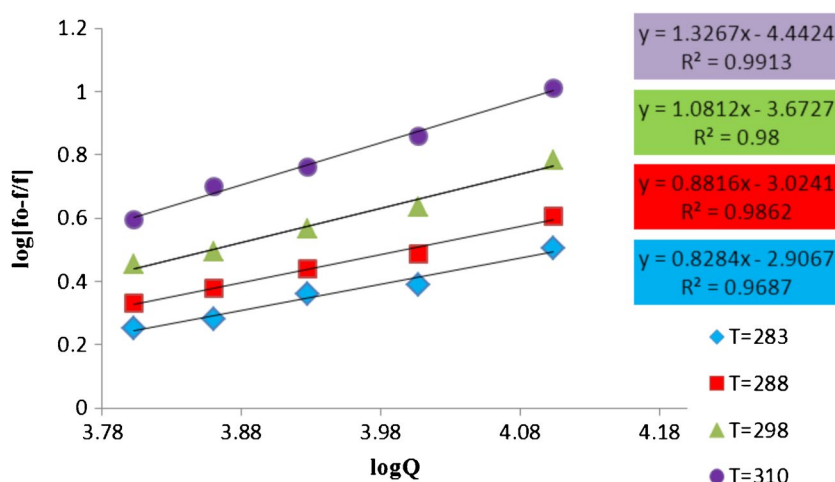


Table 2 Binding constants (K_f) and number of binding sites (n) of the DNA–ISX system

T (K)	n	Log K_f	$K_f \times 10^3$	R^2
283	0.82	2.9067	0.8	0.96
288	0.88	3.0241	1.0	0.98
298	1.08	3.6727	4.7	0.98
310	1.32	4.4424	27.6	0.99

Table 3 Thermodynamic parameters for the binding of ISX to ct-DNA

T (K)	ΔG (kJ mol ⁻¹)	ΔH (kJ mol ⁻¹)	ΔS (J mol ⁻¹ K ⁻¹)
283	-15.74		
288	-16.67		
298	-19.89	-98.72	402.55
310	-26.36		

L mol⁻¹) for dynamic quencher, suggesting that the interaction between ct-DNA and ISX happens through a static quenching mechanism [21, 22].

The apparent binding constant (K_f) and the binding stoichiometry (n) of DNA–ISX complex can be computed through the equation below [23]:

$$\log\left(\frac{F_0 - F}{F}\right) = \log K_f + n \log [Q] \tag{3}$$

In above equation, n is the number of binding sites of ct-DNA per each ISX molecule and F_0 and F are the fluorescence intensities of the fluorophore in the absence and presence of different concentrations of the ct-DNA, respectively. From fluorescence experiments, the plots of $\log(F_0 - F)/F$ against $\log[Q]$ were recorded at 283, 298, 310 K (Fig. 5) and the values of K_f and n at these temperatures are shown in Table 2.

Thermodynamic Parameters and Binding Force

The interaction forces among drug molecules and double helix of deoxyribonucleic acid (DNA) mainly consist of hydrophobic interactions, van der Waals force, hydrogen bonds and electrostatic force. To corroborate the binding force between ISX and ct-DNA, the thermodynamic

parameters at different temperatures (283, 298, 310 K) were analyzed. The binding model of drug molecules with ct-DNA can be estimated from the thermodynamic data: (1) $\Delta H < 0$ and $\Delta S > 0$, the major stabilizing forces are hydrogen bonds and hydrophobic interactions; (2) $\Delta H < 0$ and $\Delta S < 0$, the principal forces are hydrogen bonds and van der Waals forces; and (3) $\Delta H > 0$ and $\Delta S > 0$, hydrophobic interactions are the main forces [24–26]. The values of ΔH , ΔS and ΔG of the interaction between ISX and ct-DNA were determined using the Eqs. (4) and (5) shown below [27]:

$$\ln K = -\frac{\Delta H}{RT} + \frac{\Delta S}{R} \tag{4}$$

$$\Delta G = \Delta H - T\Delta S \tag{5}$$

where K is the binding constant at different temperatures (283, 298, 310 K) and R is gas constant (8.314 J mol⁻¹ K⁻¹). The values of ΔH and ΔS were gained from the slope and intercept of the linear plot (Eq. (4)) between $\ln K$ versus $1/T$. The ΔH , ΔS and ΔG values of interaction between ISX and ct-DNA are listed in Table 3. The negative value of ΔG disclose that the interaction process is spontaneous, while the negative value of ΔH and a positive ΔS value, indicate that hydrogen bonding and hydrophobic interactions have the main role in binding of drug (ISX) to ct-DNA [22].

Competitive Binding Studies

In present study on ISX-DNA interaction, the competitive fluorescence procedure was utilized. Hoechst 33258 was used as competing agent for minor groove. Also, MB and AO were used as competing agent for intercalation. Before and after addition of ISX to a mixture of ct-DNA and probe the fluorescence spectra were recorded.

As is known, Hoechst 33258 binds strongly to the minor grooves of ct-DNA with preference for adenine-thymine-rich sequences [28]. Figure 6 illustrates the fluorescence emission spectra of the fluorescence spectrum of Hoechst 33258 in Tris-HCl buffer solution. The fluorescence intensity was increased upon the addition of ct-DNA to above solution, due to binding of Hoechst 33258 to the minor grooves of DNA [29]. Remarkable quenching of fluorescence intensity was observed by addition of different amounts of ISX to the above mixture (Fig. 6), which shows the release of Hoechst to the solvent. In order to evaluate the possible interaction of ISX and Hoechst 33258, the ISX was added to the Hoechst solution and no significant

changes in the fluorescence spectrum were observed. Also, in order to verify the eventual intercalating of ISX between base pairs of DNA, methylene blue (MB) and acridine orange (AO) were used as a proper fluorophore. MB is a phenothiazinium dye that interacts with ct-DNA mainly by intercalation binding mode. Negligible changes in fluorescence intensity were observed after addition of ISX to the DNA-MB mixture (Fig. 7, Ref. [30]). These results indicate that the MB molecules are not released from ct-DNA double helix after addition of ISX. Thus the data show that the ISX is either a non-intercalator or a weaker intercalator than MB. On the other hand, insignificant changes were observed after addition of ISX to the DNA-AO mixture (Fig. 8). We note that AO is a cationic dye and can insert between two adjacent base pairs in a DNA helix [31]. The fluorescence emission spectra of AO with and without ct-DNA and the effect of ISX addition to AO bounded to ct-DNA are shown in Fig. 8. As can be seen, the fluorescence spectra indicate that there is no significant displacement of AO by ISX. Thus the results confirm the absence of an intercalative mode of binding.

Fig. 6 Fluorescence intensity of Hoechst–DNA complex in the absence and the presence of ISX. The concentration of ct-DNA and Hoechst were 9.9×10^{-5} and 5×10^{-6} mol L⁻¹, respectively, and the concentrations of ISX were 0.0, 0.49, 0.99, 1.47, 1.96, 2.43 and 2.91×10^{-5} mol L⁻¹ and pH = 7.4

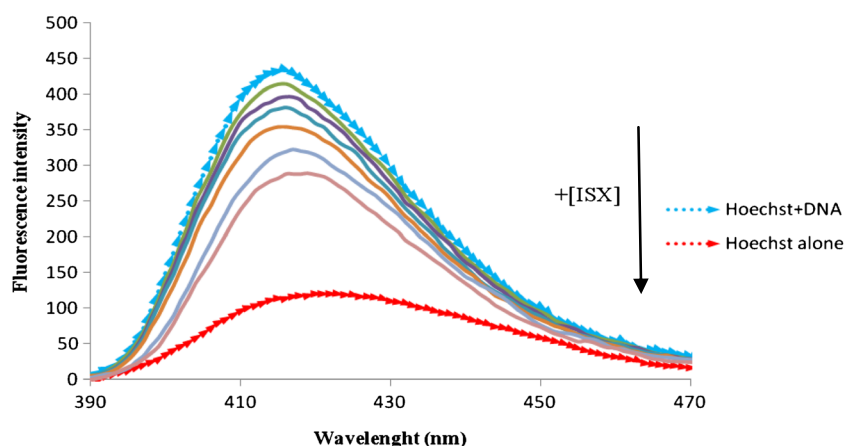


Fig. 7 Fluorescence intensity of MB–DNA complex in the absence and the presence of ISX. The concentrations of ct-DNA and MB were 12.5×10^{-5} and 5×10^{-6} mol L⁻¹, respectively, and the concentrations of ISX were 0.0, 0.49, 0.99, 1.47, 1.96, 2.43 and 2.91×10^{-5} mol L⁻¹ and pH = 7.4

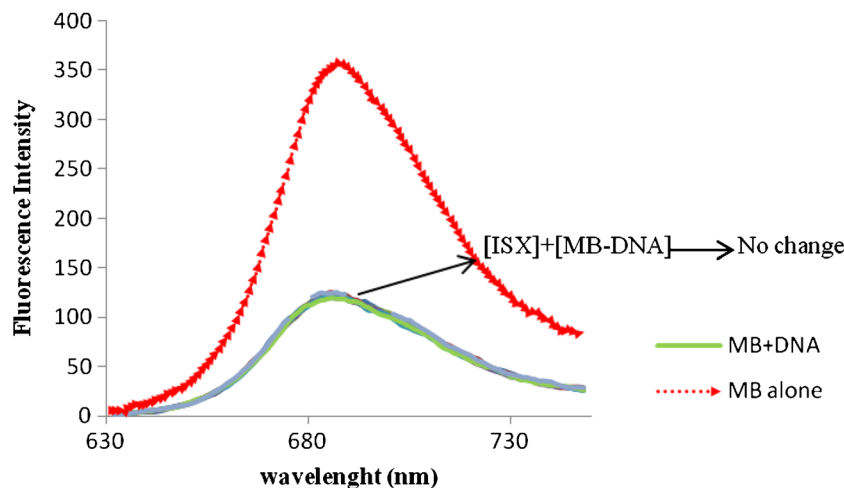
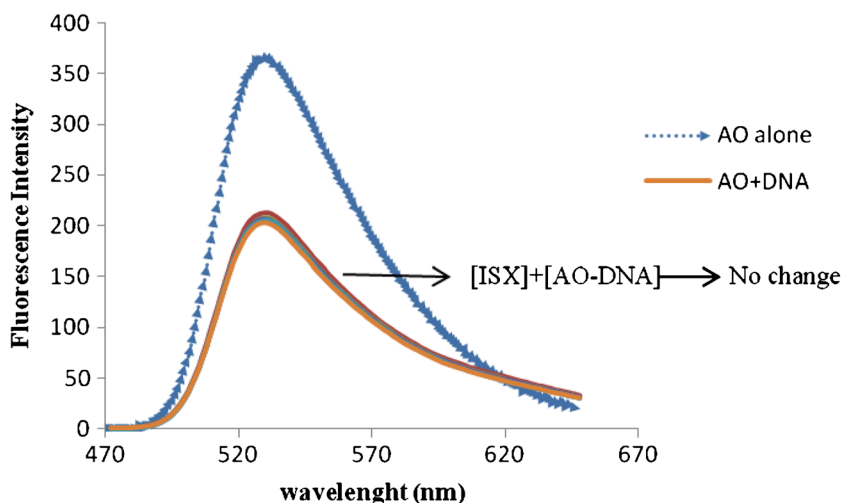


Fig. 8 Fluorescence intensity of AO–DNA complex in the absence and the presence of ISX. The concentrations of ct-DNA and AO were 7.2×10^{-5} and 5×10^{-6} mol L⁻¹, respectively, and the concentrations of ISX were 0.0, 0.49, 0.99, 1.47, 1.96, 2.43 and 2.91×10^{-5} and pH=7.4



Circular Dichroism Spectroscopy

Circular dichroism spectroscopy (CD) is widely used to analyze the structural asymmetry of small molecules. Chirality of ct-DNA can be recognized using CD spectral measurements [32].

Generally, DNA double Helix have different conformations, namely A, B, Z, etc. recognizable by its CD spectrum. The CD spectrum of ct-DNA contains a positive band at 275 nm, because of base stacking interactions and a negative band at 245 nm, due to its right-handed helicity [33]. The above bands are sensitive to binding of any drug molecules, therefore the observed changes in CD signals of ct-DNA upon on interaction with drugs may often be assigned to the corresponding changes in ct-DNA structure [34].

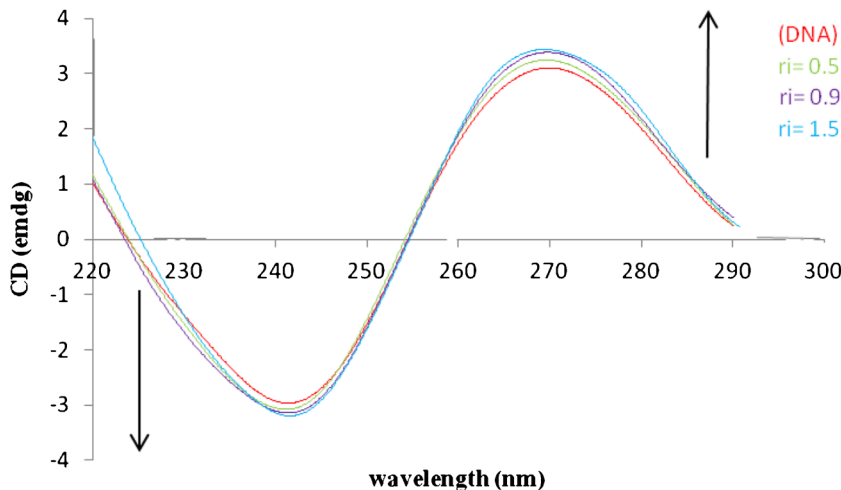
However, groove binder molecules commonly do not lead to significant unwinding of the ct-DNA base pairs [35]. The CD spectra of free ct-DNA and ct-DNA-ISX complexes are shown in Fig. 9. In the presence of ISX, the intensity of the

negative band at 245 nm and positive band at 275 nm is decreased and increased, respectively. The above observation confirms a conformational change from B to A [35], and generally happens when there is a groove binding mode of interaction [36].

Viscosity Measurements

Viscosity of deoxyribonucleic acid is susceptible to changes in the length of the DNA double helix. Accordingly the viscosity measurement is considered as one of the most critical tests for the binding mode of a drug molecule and deoxyribonucleic acid. The viscosity of the deoxyribonucleic acid solution has low changes when drug molecules bind to ct-DNA through an electrostatic or groove binding mode. However, a classical intercalator will push the affected base pairs of deoxyribonucleic acid away from each other, resulting in elongation of the double helix of ct-DNA and also increasing the relative viscosity of the solution [37–39]. If drug

Fig. 9 CD-spectra of the ct-DNA in the presence of different concentrations of ISX Conditions: c(DNA)= 8×10^{-5} mol L⁻¹; c(ISX) (1.0×10^{-4} mol L⁻¹): 0.0, 0.5, 0.9, 1.5 and pH=7.4



molecules partly intercalate into the stacked base pairs of ct-DNA, the reduction of the viscosity of the ct-DNA solution will be observed [40, 41]. The relative viscosity of ct-DNA solution upon the addition of ISX is shown in Fig. 10. As can be seen there is a slight change in the viscosity value of ct-DNA with increasing the ISX concentration, indicating that ISX mainly interacts with ct-DNA through groove mode of binding or surface binding and not intercalation mode of binding.

Effect of the Ionic Strength

Investigating the efficacy of the ionic strength on drug-DNA interactions is an efficient way to distinguish the binding modes between drug molecules and ct-DNA. The fluorescence intensity of ct-DNA–ISX solutions was monitored when NaCl solutions with different concentrations (0 to 1.3×10^{-3} mol L⁻¹) were added to the solutions (see Fig. 11). We note that NaCl salt is used to control the ionic strength of the DNA–ISX solutions. As we know, Na⁺ ions

exhibit a propensity to bind to the phosphate groups of ct-DNA via electrostatic interactions. As shown in Fig. 11, the increasing in molarity of NaCl solution has not changed significantly the emission value of ct-DNA–ISX system. Thus, we can conclude that the increasing ionic strength of solution has no significant effect on the binding between ISX and ct-DNA. The above result indicates that, at our experiment conditions, the type of ISX binding to ct-DNA is non-electrostatic.

Electrochemical Studies

Electrochemical methods can be used for studying binding interactions of electrochemically active drug molecules with deoxyribonucleic acid. The electrochemical methods enable us to appraise and auspicate DNA interactions and damage of DNA strand caused by binding of drug molecules to DNA.

As a means for further illustrating of the binding interaction between ISX and ct-DNA the differential pulse

Fig. 10 Effect of ISX on the viscosity of ct-DNA. Conditions: $c(\text{DNA}) = 5.0 \times 10^{-5}$ mol L⁻¹; $r_i = [\text{ISX}] / [\text{DNA}] = 0.0, 0.2, 0.4, 0.6, 0.8, 1, 1.2, 1.4, 1.6, 1.7, 1.9, 2, 2.2, 2.3, 2.4, 2.6, 2.7, 2.9$ and $\text{pH} = 7.4$

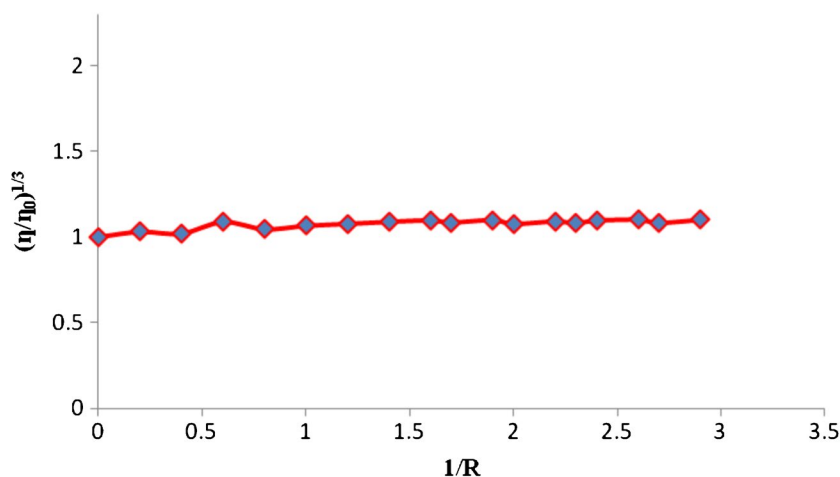
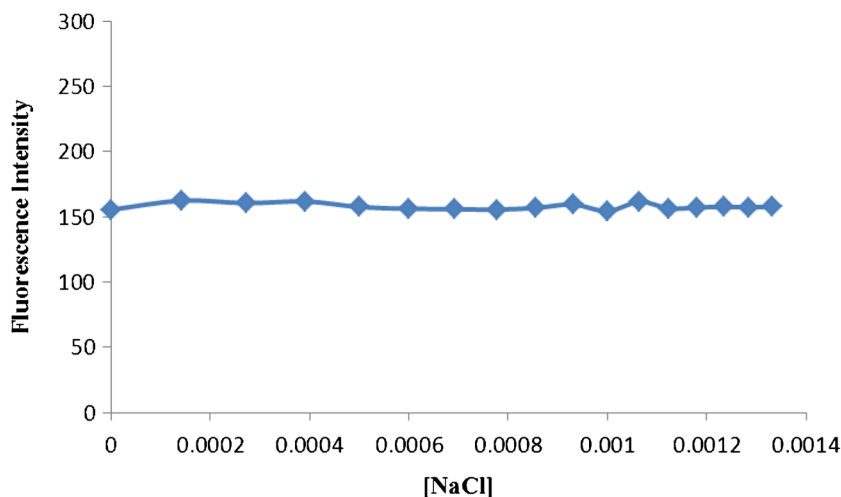


Fig. 11 Effect of ionic strength on the fluorescence intensity of ISX–DNA complex. Concentrations of ct-DNA and ISX were 3.0×10^{-5} M and 5.0×10^{-5} M, respectively



voltammograms (DPV) were studied in Tris–HCl buffer (pH 7.4). Figure 12 displays the differential pulse voltammograms of the ISX at the absence and presence of different concentrations of ct-DNA. According to Eq. (6) the positive shift of peak potential confirm interaction between ISX and ct-DNA [42] and apparent reduction in the peak currents of ISX upon the addition of ct-DNA to the solution was attributed to the diffusion of the ISX bound to the large slowly diffusing ct-DNA molecule [41].

$$E_{O/R}^0 = E_{O/R}^0 + \frac{RT}{nF} \log K_f(RY) \tag{6}$$

Where $E_{O/R}^0$ is the standard oxidation potential of ISX interacted with ct-DNA, $E_{O/R}^0$ is the standard oxidation potential of ISX, n is the number of involved electron in the oxidation, K_f is the binding constant, R , T , and F have their usual meanings.

The binding constant, K , of the interaction of ISX with ct-DNA was determined according to the Eq. (7) shown below [43]:

$$\log \left(\frac{1}{[DNA]} \right) = \log (K) + \log \left(\frac{I_{Free}}{I_{Free} - I_{Bond}} \right) \tag{7}$$

In above equation, K is the apparent binding constant and I_{Free} and I_{Bond} represent the peak current of the free guest and the adduct, respectively. According to Eq. (7), the plot of $\log(1/[DNA])$ versus $\log(I_{Free}/(I_{Free}-I_{Bond}))$ (Fig. 13) becomes linear with the intercept of $\log(K)$. Binding constants of ISX and ct-DNA were calculated to be $3.9 \times 10^3 \text{ mol}^{-1} \text{ L}$ using DPV data (Eq. 7).

Molecular Docking Studies

Molecular docking is a most important method in computer drug design [44]. The focus of molecular docking is to simulate the molecular identity process between drug molecules and DNA. Molecular docking is a helpful technique to achieve an optimized conformation for DNA and drug molecule with relative orientation between them.

Fig. 12 Differential pulse voltammogram of ISX in presence of ct-DNA at different concentrations. Conditions: $c(\text{ISX}) = 5.0 \times 10^{-5} \text{ mol L}^{-1}$, $c(\text{DNA}) (\times 10^{-5} \text{ mol L}^{-1})$: 0.0, 0.19, 0.58, 0.97, 1.3, 1.7, 2.2, 2.8, 3.7 and $\text{pH} = 7.4$

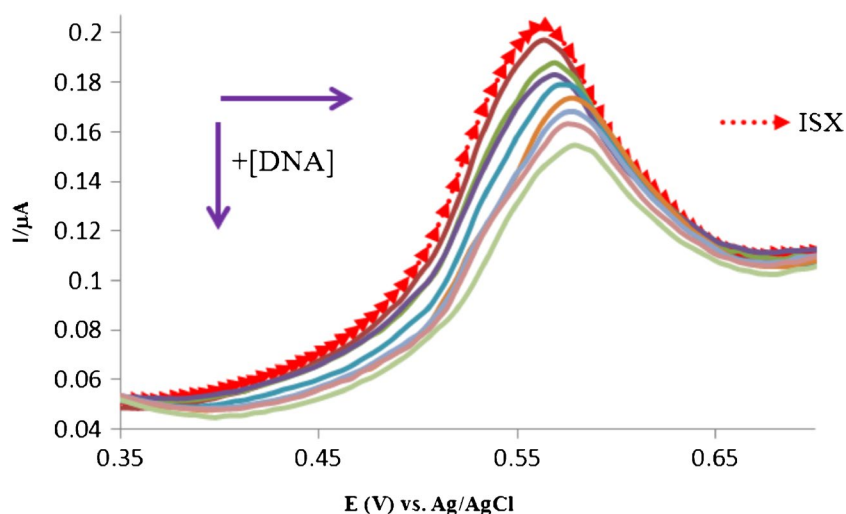


Fig. 13 Plots of $\log(1/[DNA])$ against $\log(I_{Free}/(I_{Free}-I_{Bond}))$ of ISX, in the absence and presence of different amounts of ct-DNA

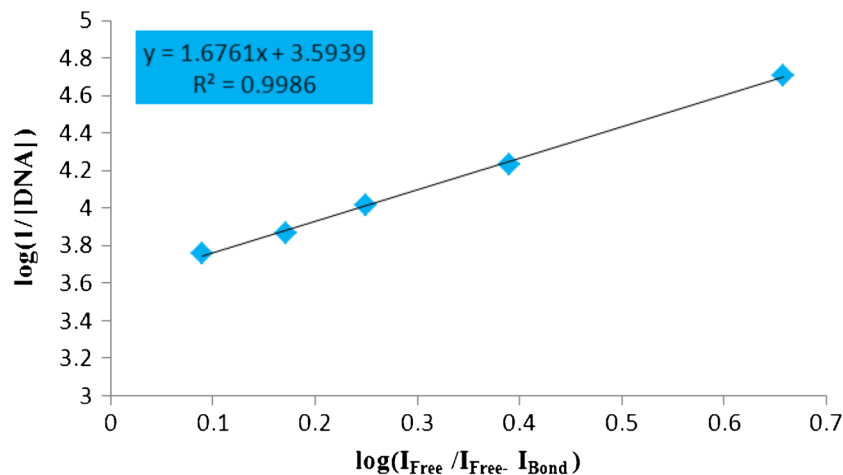
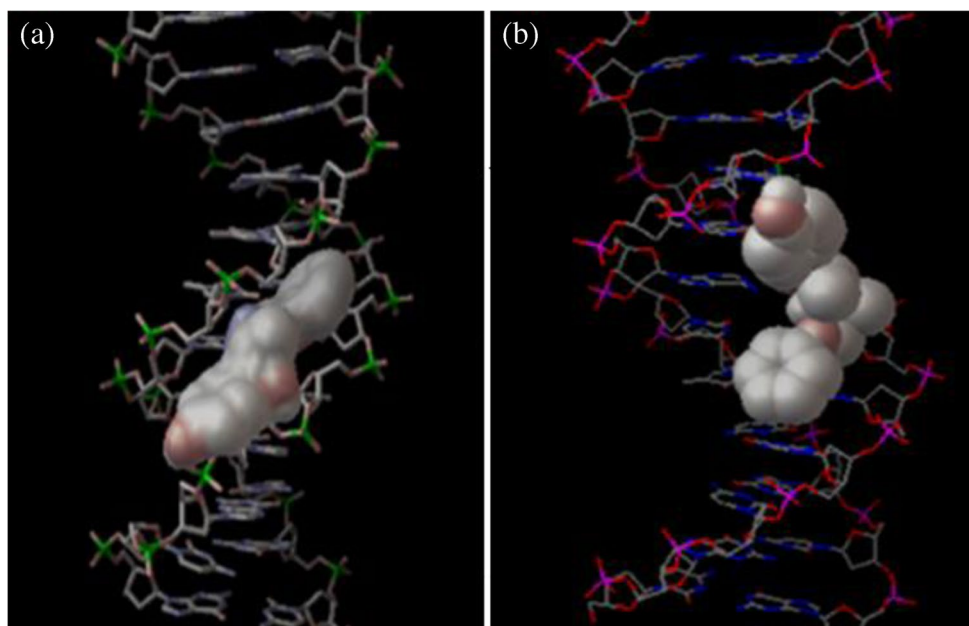


Fig. 14 Molecular docked model of ISX (a) and its protonated form (b) with DNA duplex



We note that the hydrochloride salt of ISX is used in this work and in all above discussions we have assumed that the neutral ISX have interaction with ct-DNA. Obviously, the amines and their protonated form are in equilibrium in solution. However, this is quite reliable to assume that at a buffer solution with pH of 7.4 the neutral form of amine is the dominant species. Anyway, we were interested to know if the molecular docking studies support our above logical assumption. Thus the results of spectroscopic studies were complemented with molecular docking experiments in which the ISX and its protonated form were docked to crystal structure of DNA (PDB ID: 1BNA).

The structures of the ISX and its protonated form were made flexible to attain different conformations in order to predict the best fit orientation and the best energy docked structure were analyzed. Anyway, the results show that the protonated form of ISX fits snugly into the curved contour of the targeted DNA in the major groove and not in the minor groove (Fig. 14). On the other hand, in the final docked conformation the ISX molecule occurs in a crescent shape, which is complementary to the natural curvature of the minor groove of DNA (Fig. 14). We remember that the competitive fluorimetric studies with Hoechst 33258 showed that the ISX drug exhibit the ability to displace the DNA-bound Hoechst 33258, indicating that it binds to the minor groove of ct-DNA. Thus, the molecular docking studies clearly support our spectroscopic studies and also this assumption that mainly the neutral ISX, and not its protonated form, binds to ct-DNA.

Conclusions

In this work, the interaction of ISX with ct-DNA was investigated using electronic absorption spectroscopy, circular dichroism (CD), fluorescence spectroscopy, viscosity measurement and molecular docking. Fluorescence quenching shows the binding between ISX and ct-DNA occurs through static quenching mechanism. Thermodynamic parameters (enthalpy and entropy) suggested that hydrogen bonds and hydrophobic interactions play an important role in binding process. The molecular docking of the ISX with the DNA duplex demonstrates that ISX prefers to bind in the AT-rich minor grooves of ct-DNA. The data show that the ISX has induced some slight changes in the CD spectrum of ct-DNA and has a little effect on the viscosity of ct-DNA.

Acknowledgements The financial support from Bu-Ali Sina University Research Center is gratefully acknowledged.

Compliance with Ethical Standards

Conflict of Interest The authors declare that they have no conflict of interest.

References

1. Shahabadi N, Fili SM, Kheiridoosh F (2013) Study on the interaction of the drug mesalamine with calf thymus DNA using molecular docking and spectroscopic techniques. *J Photochem Photobiol B Biol* 128:20–26

- Dogra S, Awasthi P, Nair M, Barthwal R (2013) Interaction of anticancer drug mitoxantrone with DNA hexamer sequence d-(CTCGAG)₂ by absorption, fluorescence and circular dichroism spectroscopy. *J Photochem Photobiol B Biol* 123:48–54
- Charak S, Mehrotra R (2013) Investigation of idarubicin–DNA interaction: Spectroscopic and molecular docking study. *Int J Biol Macromol* 60:213–218
- Gua T, Hasebe Y (2012) Novel amperometric assay for drug–DNA interaction based on an inhibitory effect on an electrocatalytic activity of DNA–Cu(II) complex. *Biosens Bioelectron* 33:222–227
- Williams AK, Dasilva SC, Bhatta A, Rawal B, Liu M, Korobkova EA (2012) Determination of the drug–DNA binding modes using fluorescence-based assays. *Anal Biochem* 422:66–73
- Balakrishnan S, Jaldappagari S (2013) Binding of an anticancer Rutaceae plant flavonoid glycoside with calf thymus DNA: biophysical and electrochemical studies. *J Lumin* 142:17–22
- Patel MN, Dosi PA, Bhatt BS (2012) Interaction of palladium(II) coordination compounds with calf thymus DNA and their antibacterial activity. *Inorg Chem Commun* 21:61–64
- Singh MP, Joseph T, Kumar S, Bathini Y, Lown JW (1992) Synthesis and sequence-specific DNA binding of a topoisomerase inhibitory analog of Hoechst 33258 designed for altered base and sequence recognition. *Chem Res Toxicol* 5:597–607
- Sparks J, Scholz C (2009) Evaluation of a cationic poly(β -hydroxyalkanoate) as a plasmid DNA delivery system. *Biomacromolecules* 10:1715–1719
- Lown JW (1998) *Anticancer Drug Des* 3:25–40
- Reynolds JEF (ed) (1996) *Martindale: the extra pharmacopoeia*, 31st edn. The Pharmaceutical Press, London
- Becke AD (1988) Density-functional exchange-energy approximation with correct asymptotic behavior. *Phys Rev A* 38:3098–3100
- Perdew JP (1986) Density-functional approximation for the correlation energy of the inhomogeneous electron gas. *Phys Rev B* 33:8822–8824
- Weigend F, Ahlrichs R (2005) Balanced basis sets of split valence, triple zeta valence and quadruple zeta valence quality for H to Rn: design and assessment of accuracy. *Chem Phys* 7:3297–3305
- Frisch MJ, Trucks GW, Schlegel HB, Scuseria GE, Robb MA, Cheeseman JR, Montgomery JAJ, Vreven T, Kudin KN, Burant JC, Millam JM, Iyengar SS, Tomasi J, Barone V, Mennucci B, Cossi M, Scalmani G, Rega N, Petersson GA, Nakatsuji H, Hada M, Ehara M, Toyota K, Fukuda R, Hasegawa J, Ishida M, Nakajima T, Honda Y, Kitao O, Nakai H, Klene M, Li X, Knox JE, Hratchian HP, Cross JB, Adamo C, Jaramillo J, Gomperts R, Stratmann RE, Yazyev O, Austin AJ, Cammi R, Pomelli C, Ochterski JW, Ayala PY, Morokuma K, Voth GA, Salvador P, Dannenberg JJ, Zakrzewski VG, Dapprich S, Daniels AD, Strain MC, Farkas O, Malick DK, Rabuck AD, Raghavachari K, Foresman JB, Ortiz JV, Cui Q, Baboul AG, Clifford S, Cioslowski J, Stefanov BB, Liu G, Liashenko A, Piskorz P, Komaromi I, Martin RL, Fox DJ, Keith T, Al-Laham MA, Peng CY, Nanayakkara A, Challacombe M, Gill B, Johnson PMW, Chen W, Wong MW, Gonzalez C, Pople JA (2003) Gaussian software. Gaussian Inc, Pittsburgh
- Morris GM, Goodsell DS, Halliday RS, Huey R, Hart WE, Belew RK, Olson AJ (2007) Autodock version 4.0.1. The Scripps Research Institute, La Jolla
- Morris GM, Goodsell DS, Halliday RS, Huey R, Hart WE, Belew RK, Olson AJ (1998) Automated docking using a Lamarckian genetic algorithm and an empirical binding free energy function. *J Comput Chem* 19:1639–1662
- Morris GM, Huey R, Lindstrom W, Sanner MF, Belew RK, Goodsell DS, Olson AJ (2009) Auto dock 4 and auto dock tools 4: automated docking with selective receptor flexibility. *J Comput Chem* 30:2785–2791
- Wolfe A, Shimer GH, Meehan T (1987) Polycyclic aromatic hydrocarbons physically intercalate into duplex regions of denatured DNA. *Biochemistry* 26:6392–6396
- Jalali F, Rasae G (2015) Electrochemical, spectroscopic, and theoretical studies on the interaction between azathioprine and DNA. *Int J Biol Macromol* 81:427–434
- Wu Y, Yang G (2010) Interaction between garcigenin and DNA by spectrophotometry and fluorescence spectroscopy. *Spectrosc Lett* 43:28–35
- Tao M, Zhang G, Pan J, Xiong C (2016) Deciphering the groove binding modes of tau-fluvalinate and flumethrin with calf thymus DNA. *Spectrochim Acta A* 155:28–37
- Li JF, Dong C (2009) Study on the interaction of morphine chloride with deoxyribonucleic acid by fluorescence method. *Spectrochim Acta A* 71:1938–1943
- Ross PD, Subramanian S (1981) Thermodynamics of protein association reactions: forces contributing to stability. *Biochemistry* 20:3096–3102
- Yuan JL, Liu H, Kang X, Lv Z, Zou GL (2008) Characteristics of the isomeric flavonoids apigenin and genistein binding to hemoglobin by spectroscopic methods. *J Mol Struct* 891:333–339
- Kashanian S, Ezzati Nazhad Dolatabadi J (2009) In vitro study of calf thymus DNA interaction with butylated hydroxyanisole. *DNA Cell Biol* 28:535–540
- Zhang GW, Wang LH, Zhou XY, Li Y, Gong DM (2014) Binding characteristics of sodium saccharin with calf thymus DNA in vitro. *J Agric Food Chem* 62:991–1000
- Kakkar R, Garg R (2002) Theoretical study of tautomeric structures and fluorescence spectra of Hoechst 33258. *J Mol Struct THEOCHEM* 579:109–113
- Guan Y, Zhou W, Yao X, Zhao M, Li Y (2006) Determination of nucleic acids based on the fluorescence quenching of Hoechst 33258 at pH 4.5. *Anal Chim Acta* 570:21–28
- Rasae G, Jalali F (2015) Electrochemical, spectroscopic, and theoretical studies on the interaction between azathioprine and DNA. *Int J Biol Macromol* 81:427–434
- Bi S, Qiao C, Song D, Tian Y, Gao D, Sun Y, Zhang H (2006) Study of interactions of flavonoids with DNA using acridine orange as a fluorescence probe. *Sensors Actuators B* 119:199–208
- Rodger A (1997) *Circular dichroism and linear dichroism*. Wiley Online Library
- Ivanov V, Minchenkova L, Schyolkina A, Poletayev A (1973) Different conformations of double-stranded nucleic acid in solution as revealed by circular dichroism. *Biopolymers* 12:89–110
- Lincoln P, Tuite E, Norden B (1997) Short-circuiting the molecular wire: cooperative binding of Δ -[Ru(phen)₂dppz]²⁺ and Δ -[Rh(phi)₂bipy]³⁺ to DNA. *J Am Chem Soc* 119:1454–1455
- Rehman SU, Sarwar T, Husain MA, Ishqi HM, Tabish M (2015) Studying non-covalent drug–DNA interactions. *Arch Biochem Biophys* 576:49–60
- Li FH, Zhao GH, Wu HX, Lin H, Wu XX, Zhu SR, Lin HK (2006) Synthesis, characterization and biological activity of lanthanum(III) complexes containing 2-methylene-1,10-phenanthroline units bridged by aliphatic diamines. *J Inorg Biochem* 100:36–43
- Satyanarayana S, Dabrowiak JC, Chaires JB (1992) Neither Δ -nor Λ -tris(phenanthroline)ruthenium(II) binds to DNA by classical intercalation. *Biochemistry* 31:9319–9324
- Lincoln P, Norden B (1998) DNA binding geometries of ruthenium(II) complexes with 1,10-phenanthroline and 2,2'-bipyridine ligands studied with linear dichroism spectroscopy. Borderline cases of intercalation. *J Phys Chem B* 102:9583–9594
- Bielawski K, Bielawska A, Anchim T, Wolczynski S (2005) Synthesis, DNA binding, topoisomerase inhibition and cytotoxic properties of 2-chloroethylnitrosourea derivatives of hoechst 33258. *Biol Pharm Bull* 28:1004–1009

40. Zhou X, Zhang G, Pan J (2015) Groove binding interaction between daphnetin and calf thymus DNA. *Int J Biol Macromol* 74:185–194
41. Fei Y, Lu G, Fan G, Wu Y (2009) Spectroscopic studies on the binding of a new quinolone antibacterial agent: sinifloxacin to DNA. *Anal Sci* 25:1333–1338
42. Bard AJ, Faulkner LR (2001) *Electrochemical methods*, second edn. Wiley, New York, p 36
43. Feng Q, Li NQ, Jiang YY (1997) Electrochemical studies of porphyrin interacting with DNA and determination of DNA. *Anal Chim Acta* 344:97–104
44. El-Sonbati AZ, Mohamed GG, El-Bindary AA, Hassan WMI, Diab MA, Morgan SM, Elkholy AK (2015) Supramolecular structure, molecular docking and thermal properties of azo dye complexes. *J Mol Liq* 212:487–502